Proceedings of ASME Turbo Expo 2013: Turbine Technical Conference and Exposition
GT2013
June 3-7, 2013, San Antonio, Texas, USA

GT2013-94425

WINGLETS FOR IMPROVED AEROTHERMAL PERFORMANCE OF HIGH PRESSURE TURBINES

John D. Coull, Nick R. Atkins, Howard P. Hodson
Whittle Laboratory, University of Cambridge, UK

ABSTRACT

This paper investigates the design of winglet tips for unshrouded high pressure turbine rotors, considering aerodynamic and thermal performance simultaneously. A novel parameterization method has been developed to alter the tip geometry of a rotor blade. A design survey of un-cooled, flat-tipped winglets is performed using RANS calculations for a single rotor at engine representative operating conditions.

Compared to a plain tip, large efficiency gains can be realized by employing an overhang around the full perimeter of the blade, but the overall heat load rises significantly. By employing an overhang on only the early suction surface, significant efficiency improvements can be obtained without increasing the overall heat transfer to the blade.

The flow physics are explored in detail to explain the results. For a plain tip, the leakage and passage vortices interact to create a three-dimensional impingement onto the blade suction surface, causing high heat transfer. The addition of an overhang on the early suction surface displaces the tip leakage vortex away from the blade, weakening the impingement effect and reducing the heat transfer on the blade. The winglets reduce the aerodynamic losses by unloading the tip section, reducing the leakage flow rate, turning the leakage flow in a more streamwise direction and reducing the interaction between the leakage fluid and endwall flows. Generally these effects are most effective close to the leading edge of the tip, where the leakage flow is subsonic.

1 INTRODUCTION

The design of rotor blade tips for unshrouded High Pressure (HP) turbines is a complex multi-objective process. The designer has to minimize the aerodynamic losses induced by the flow leaking through the tip gap, while lessening the heat transfer between the hot gases and the blade. In addition the geometry must allow for sufficient internal and external cooling, satisfy stress and life requirements, and allow for reasonable performance retention in service. Given these complexities it is unsurprising that considerable research has been devoted to HP turbine tip design over many decades. Most of the fundamental studies of tip flows have involved low Mach number testing ([1] [2]), but it has been shown that at engine conditions large regions of the tip flow are supersonic and exhibit very different flow behavior ([3], [4], [5]). Therefore it is important that compressibility effects are correctly accounted for.

1.1 Flow in the tip gap

Fundamentally, the tip leakage flow is driven by the pressure difference between the pressure and suction sides of the blade, P_p and P_s. One may consider a control volume covering a small section of the tip gap, as shown in Fig. 1. Slow moving fluid on the blade pressure surface is drawn up the blade and into the tip gap, typically separating on the edge at subsonic speeds. The resultant separation bubble reduces the effective flow area of the tip gap, tending to restrict the leakage mass flow. The separation may or may not reattach, depending on the local ratio of blade thickness to gap height, t/τ, the Reynolds number and the Mach number [4]. The effective sealing of the tip gap may be locally quantified using the discharge coefficient C_D:

$$C_D = \frac{\dot{m}_{cv}}{\dot{m}_{cv-is}} \tag{1}$$

were $\dot{m}_{cv}$ is the mass flow rate through the control volume and $\dot{m}_{cv-is}$ is its isentropic value. The discharge coefficient captures the influence of the flow separation and reattachment, if present, and the influence of the relative casing motion, which acts to reduce the leakage mass flow rate (Fig. 1).

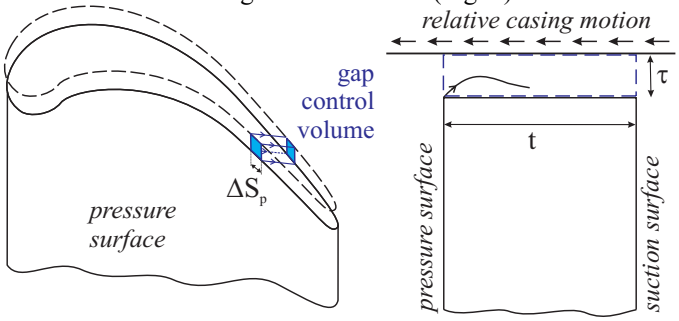

Fig. 1 Left: control volume for a section of the tip gap; right: cross-section normal to the local pressure surface.

Copyright © 2013 by ASME

For incompressible flow without streamtube contraction, the mass flow through the control volume in Fig. 1 is simply:

$$\dot{m}_{cv} = C_D \, \tau \, \Delta S_p \sqrt{2\rho (P_p - P_s)} \qquad (2)$$

where τ is the tip gap height and ΔS_p is the width of the control volume parallel to the local pressure surface edge. This equation is valid because it can be reasonably assumed that the streamwise momentum on the pressure side of the tip gap is preserved as the flow passes through the gap. At high speeds the effects of compressibility must also be considered. The Mach number M_{N-is} and mass flow rate $\dot{m}_{cv-is}$ through the tip gap are given by:

$$M_{N-is} = \min\left[\left(\frac{2}{\gamma - 1} \right) \left(\left(\frac{P_S}{P_P} \right)^{\frac{\gamma-1}{\gamma}} - 1 \right), 1 \right] \qquad (3)$$

$$\dot{m}_{cv-is} = \frac{\tau \Delta S_p P_p}{\sqrt{C_p T_p}} \frac{\gamma}{\sqrt{\gamma - 1}} M_{N-is} \left(1 + \frac{\gamma - 1}{2} {M_{N-is}}^2 \right)^{-\frac{1}{2}\left(\frac{\gamma+1}{\gamma-1}\right)} \qquad (4)$$

The maximum mass flow rate through the tip gap is limited by choking. Compressibility also strongly affects the flow physics of the reattachment and heat transfer processes. At low Mach numbers the reattachment of the pressure side separation bubble causes the flow to decelerate, resulting in an amplification of turbulence and high heat transfer rates on the tip surface [1]. At high Mach numbers the flow accelerates strongly downstream of the throat in the gap, expanding as it does so and thus forcing the flow to re-approach the surface. This acceleration acts to reduce the turbulence intensity and hence the heat transfer coefficients on the tip. In addition the recovery temperature of the gas reduces in the high Mach number regions, decreasing the temperature gradient driving the heat transfer. These effects are partially counteracted by locally enhanced heat transfer rates induced by interactions between the shocks and the tip boundary layer.

1.2 Impact on aerodynamic performance

On exiting the suction side of the tip gap, the leakage flow emerges into the passage and typically rolls up to form a vortex. This fluid is under-turned relative to the freestream and so the presence of the tip gap reduces the power output from the rotor. The aerodynamic losses rise due to a combination of:

1. Entropy generation inside the tip gap, which tends to reduce the leakage flow rate;
2. Mixing of the tip leakage flow with the freestream gas;
3. Interaction with the passage secondary flows.

Simple control volume modeling of the first two mechanisms has previously been proposed, e.g. [6], [7], [8]. The third mechanism occurs because the leakage and passage vortices tend to reinforce one another ([2]).

1.3 Controlling tip leakage flow with winglets

Many strategies have been proposed for reducing the losses caused by the tip leakage flow, which are of particular significance when one considers that in-service deterioration tends to open up the tip gap and increase these losses. Arguably the "best" aerodynamic solution is to employ a fixed shroud on the tip, allowing multiple knife-seals and turning fins to be employed [2]. For unshrouded blades a common approach is to employ a cavity on the tip, causing a second separation to form over the suction surface wall, improving the sealing and reducing the discharge coefficient. Other potential tip strategies include modifying the three-dimensional design of the blade, either to off-load the tip of the blade ([2]) or to locally front-load the profile ([9]). This paper examines another strategy, namely to employ a winglet on the blade tip that overhangs into the passage. In principle such winglet tips reduce the driving pressure ratio across the gap and hence the leakage mass flow.

Most of the reported winglet investigations have been performed using low speed cascade tests and are therefore only of limited relevance to real engines. Many of the published investigations show mixed or conflicting results ([2]). The design problem may be further complicated by the inclusion of cavities and squealers on winglet tips, as studied by several authors (e.g. [10], [11], [12], [13], [14]).

Many winglet investigations have focused on aerodynamic performance alone, yet winglets increase the blade surface area and therefore tend to increase the overall heat transfer. While some recent studies have presented both aerodynamic and thermal measurements on winglet tips (e.g. [14] [15]), the heat transfer penalties relative to plain tips have not been detailed.

This paper examines the winglet design space, with a view to maximizing aerodynamic efficiency while minimizing heat transfer. An attempt has been made to keep the study as simple as possible to aid the interpretation of the results:

- The paper considers a design study of flat-tipped winglets applied to a rotor blade. In practice designers may consider adding a cavity to such designs, but the simpler geometry of the flat tip is sufficient to demonstrate the effect of the overhangs.
- Cooling is not considered. The intricacies of internal and external cooling are beyond the scope of this investigation.
- A simplified inlet boundary condition is used for most of the calculations; a sensitivity study shows that similar results are obtained for more realistic conditions.

The subsequent sections outline the methods employed, examine the overall performance of several designs and analyze the flow behavior to explain the results.

2 NOMENCLATURE

2.1 Symbols

A	area
C_x	axial chord
C_D	discharge coefficient (equation (1))
h	heat transfer coefficient
k	conductivity at wall temperature
$\dot{m}$	mass flow rate
M	Mach number
Nu	Nusselt number $= h C_x / k$
P	pressure

Copyright © 2013 by ASME

q	heat flux (W/m^2)
$\dot{s}_{mix}$	entropy generation rate due to mixing
S	surface length
t	local blade thickness
T , T_{wall}	temperature, wall temperature
γ	ratio of specific heat capacities
η	isentropic rotor efficiency
θ	angle between the leakage and freestream
ρ	density
τ , τ^*	tip gap, tip gap as a fraction of span

2.2 Subscripts

cv	control volume
is	isentropic
N	component normal to pressure surface
p , s	pressure surface, suction surface

3 COMPUTATIONAL METHODS

3.1 Geometry Parameterization

A method of parameterising flat-tipped winglet geometries has been developed in MatLab. The code is designed to allow freedom in the design space while minimizing the number of parameterization variables. Starting with the definition of the datum plain tip blade, the two-dimensional shape of the winglet is generated by applying a variable overhang around the tip. The size of the overhang is controlled by the series of control points illustrated in Fig. 2. In this study the trailing edge overhangs were set to zero to maintain a constant trailing edge thickness, and so the designs considered have six degrees of freedom. The three-dimensional geometry is generated by imposing a blending function between the winglet tip and the baseline blade. In this paper, the winglet tips are blended into the blade geometry at an angle of 45°, and the join between the winglet and blade is smoothed to avoid any discontinuities on the blade. The edges of the blade tip are sharp. The blade and domain geometry is defined as a series of NURB surfaces, as shown in Fig. 3, and exported as an IGES CAD file.

3.2 Meshing and CFD

The CFD reported in this paper have been performed on the single rotor domain shown in Fig. 4. Unstructured meshes were generated using Centaur v9.0.2. This approach has several advantages over structured meshing for the current application, including the ease of automation and the ability to concentrate the mesh points in the region of the tip gap.

Computations were performed using the CFX5 v12.1 commercial software package. CFX is an implicit pressure-based solver which uses a coupled approach to solve the Reynolds-Averaged Navier-Stokes (RANS) equations. The current calculations use the high-resolution (second order) advection scheme. Turbulence was modeled with the 2-equation SST model. Boundary layers were modeled as fully turbulent, since the extent of laminar flow in the tip gap is expected to be small. A constant wall temperature was specified, giving a gas to wall ratio of approximately 1.5 which is considered broadly representative of real engine conditions. Profiles of total pressure, temperature and flow angle consistent with an engine through-flow calculation were applied at the inlet, and an area-averaged pressure at the outlet. Relatively coarse inlet boundary conditions (see Fig. 21) have been employed to simplify the analysis of the flow-field and aid understanding of the physics; a sensitivity study in section 6.7 shows that similar performance benefits are found when a more detailed traverse is applied.

Coolant flows have not been modeled in this study.

3.3 Normalized Change in Heat Load

Since the addition of a winglet changes the area of the blade surface as well as the tip, it is necessary to consider heat transfer changes over the whole blade. Relative to the datum plain tip design at a tip gap of 1% of span, the normalized change in heat load ΔH^* is defined as the change in heat load over the whole blade surface, divided by the heat load on the tip surface for the datum case:

$$\Delta H^* = \frac{\int_{blade\&tip} q\,dA - \int_{DATUM\ blade\&tip} q\,dA}{\int_{DATUM\ tip} q\,dA} \qquad (5)$$

Normalizing in this manner ensures that ΔH^* is largely independent of the aspect ratio of the blade. The use of a global integral of this form neglects the importance of localized hot spots, as well as the relative difficultly of cooling different parts

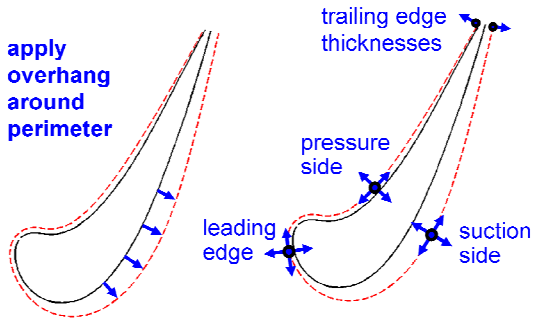

Fig. 2 Parameterization of the winglet tip shape.

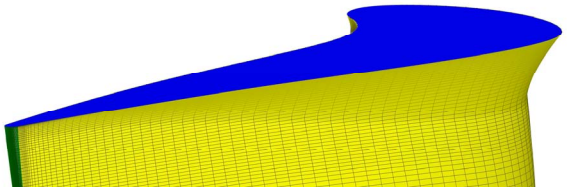

Fig. 3 NURB representation of a sample geometry, showing the three-dimensional blending.

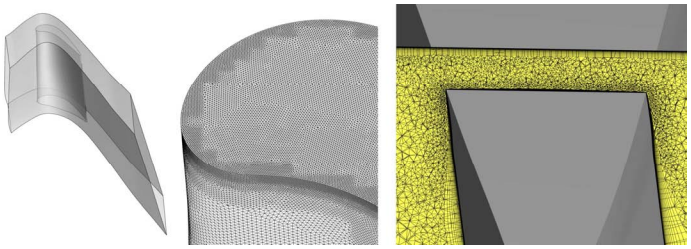

Fig. 4 Domain and mesh, datum plain tip, 1% tip gap.

Copyright © 2013 by ASME

of the blade. However the peak heat flux values were similar for all of the designs and therefore this global approach is a reasonable, if simplistic, method of comparing designs.

3.4 Equivalent Adiabatic Rotor Efficiency

Since a representative wall temperature is maintained during the simulations, heat is extracted from the working fluid and consequently the standard definition of adiabatic efficiency cannot be employed. An equivalent adiabatic efficiency for the rotor alone was calculated from mass-averaged inlet and exit quantities using the method of Atkins and Ainsworth [16], which accounts for both first and second-law corrections.

3.5 Mesh Sensitivity

The influence of mesh density on the calculated efficiency and blade heat load is presented in Fig. 5 for the datum plain tip at a tip gap of 1% of span. The vertical axis shows the change in efficiency $\Delta\eta$ for each case; the horizontal axis shows the normalized change in heat load $\Delta H*$. With the exception of the coarsest mesh, the predicted efficiencies lie within 0.15% of each other and $\Delta H*$ within 0.12. The finer meshes with more

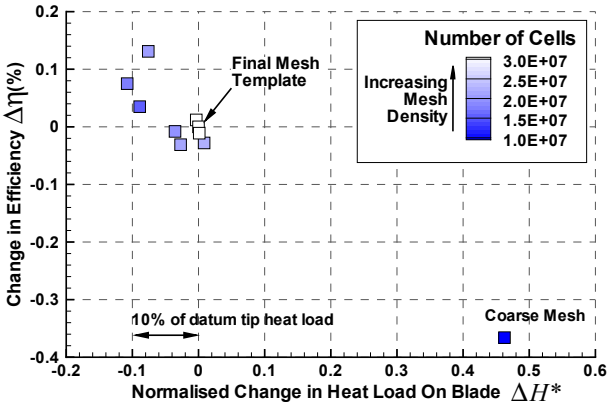

Fig. 5 Dependency of heat load and efficiency on mesh density, for a tip gap of 1% of span.

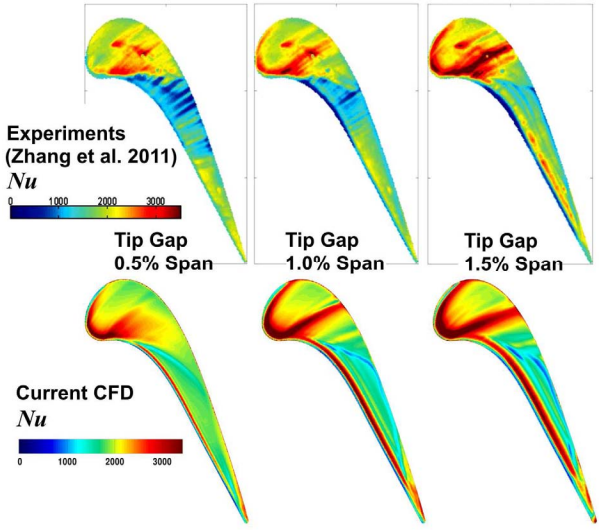

Fig. 6 High-speed cascade heat transfer at three tip gaps: top, experiments [10]; bottom, computations.

than 25 million cells (white-filled symbols) showed a maximum efficiency variation of 0.03% and a normalized heat load variation of 0.01. Note that a high mesh density is required because of the high Reynolds number and Mach numbers of the flow. The final mesh for the plain tip case is illustrated in Fig. 4, which has around 60-70 points across the tip gap and y^+ approximately equal to unity on both the blade tip and on the casing within the tip gap. The input parameters for this mesh were used for all of the cases in this paper.

3.6 Experimental Validation

To assess the accuracy of the CFD methods, calculations were performed for the high-speed linear cascade reported by Zhang et al. [10] and O'Dowd et al. [11]. Experimental and computed heat transfer coefficients for tip gaps of 0.5%, 1.0% and 1.5% of span are presented in Fig. 6. Over the front portion of the surface, the experiments show a region of high heat transfer where the flow undergoes subsonic reattachment. As the tip gap opens this region grows in size, forming a distinct horseshoe shape, and the heat transfer coefficients rise. The CFD simulations reproduce these features and the variation with tip gap. Further aft on the blade the Mach numbers in the tip gap reach supersonic speeds. The measured heat transfer coefficients in this region are generally low due to the high acceleration which damps the turbulence. Also evident in the experiments are lines of moderately high heat transfer caused by the reattachment of the pressure surface separation; the heat transfer in these regions increases as the gap opens. The CFD generally over-predicts the heat transfer coefficients in this region, especially for the lower tip gaps, which may be a result of insufficient dissipation in the turbulence model. In addition, the tip edges of the manufactured cascade blades will have an unknown finite radius, which will reduce the severity of the pressure surface separation compared to the sharp edges used in the CFD. A similar over-prediction was observed in the calculations performed by Zhang et al. [10] using the SA turbulence model. Despite the over-prediction in this region, the overall comparison is favorable since the CFD captures the correct flow physics and the changes as the tip gap opens.

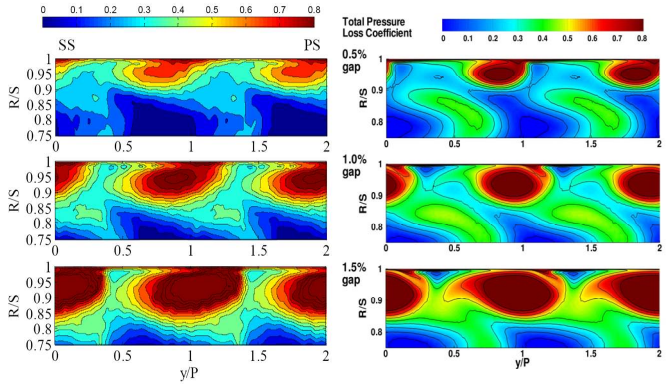

Fig. 7 High-speed cascade loss coefficients for three tip gaps. Left: experiments [11]; right: computations.

Copyright © 2013 by ASME

以上内容仅为本文档的试下载部分，为可阅读页数的一半内容。如要下载或阅读全文，请访问：https://d.book118.com/025312103100011310